In Proceedings of the 13th International Detonation Symposium, pp. 1035–1044.

EXPLOSIVE-DRIVEN SHOCK WAVES IN ARGON

W. C. Davis, T. R. Salyer, S. I. Jackson, and T. D. Aslam
Los Alamos National Laboratory
Los Alamos, New Mexico 87545

Revision 6/30/2006

Abstract. Strong shock waves propagating in argon gas exhibit a variety of precursor effects. The main shock wave appears to be unstable and supports perturbations ahead of it that are fed by radiation or other energy from the main front. Confining walls oriented parallel to the shock motion absorb radiation from the shock front and produce a heated region near the wall that supports perturbations consisting of oblique shock waves, which precede the main shock. A bright region exists where the oblique and main shocks intersect due to elevated temperatures from shock focusing. Perturbations in the form of small floating drops are also found to propagate ahead of the main shock. Wires with their long axis in the direction of the flow also support a hot thermal boundary layer, causing a shock wave to run far ahead of the main shock in a similar fashion to the oblique shocks on the confining walls. These precursor effects are presented and discussed.

INTRODUCTION

Shock-heated argon is often used as an extremely bright light source for high-speed photography of fast-acting experiments, such as explosive devices. A typical argon flash, shown in Fig. 1, consists of a tube filled with argon gas. A window is located at one end and a high explosive (HE) charge is located at the other. Detonation of the explosive sends a shock wave into the argon. The temperatures and pressures behind the shock front are sufficient to excite the argon gas to the point that it emits electromagnetic radiation in the visible and ultraviolet parts of the spectrum. This light travels through the window and illuminates the target. These sources have had many forms and have also been referred to as argon bombs, argon candles, and argon light sources.

Since most detectors used have only measured a limited range of wavelengths, brightness levels measured are typically reported as those that a blackbody would emit over the wavelength range measured. Published values range from 15,000 K to 30,000 K, with the best values around 25,000 K. This large range is partly due to the different strengths of

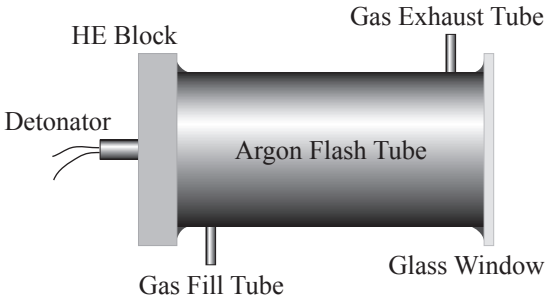

FIGURE 1. An example of an argon flash.

the explosive drivers used to create the argon flashes, as well as to uncertainties in the wavelength response of the detectors and the difficulty of finding a calibration source. To date, most brightness measurements have been made in the visible spectrum, with some in the near ultraviolet (200–380 nm). No data is available for emission brightness in the hard ultraviolet (10–200 nm) even though the peak of the blackbody curve for the aforementioned temperature values ranges from 97–193 nm. In this paper we discuss some observations of effects that may be due to the hard ultraviolet (UV).

The state of a shock driven by explosive is determined by the intersection of the Hugoniot curve for

Approved for unlimited release: LA-UR-06-4493

In Proceedings of the 13th International Detonation Symposium, pp. 1035–1044.

the shocked material and the expansion isentrope of the explosive products. When the shocked material is a gas at ambient pressure, its Hugoniot curve intersects the isentrope at very low pressure, so the particle speed U_p is near the escape speed for the products and varies only mildly from one gas to another. The internal energy E is approximated by $E - E_0 = \frac{1}{2}U_p$ and is nearly the same for any gas. The temperature of the gas then depends mostly on its specific heat. The noble gases argon, krypton, and xenon have very small specific heats and thus are shocked to high temperatures. The specific heat depends approximately on $M^{-\frac{1}{2}}$ where M is the atomic mass, so for a given shock strength the temperature is lower for argon than for heavier gases like krypton and xenon. Argon is usually used because it is much less expensive than the other two.

Argon at ambient conditions is transparent over a wide span of ultraviolet wavelengths, allowing ultraviolet radiation from the shocked gas to reach all parts of any confining tube or box. This radiation has been observed to interact with various surfaces to produce unexpected phenomena. Most of the phenomena are innocuous, such as the appearance of "floating drops" ahead of the shock front or the growth of boundary disturbances ahead of the main front. However the radiation from the shocked gas has also been observed to heat a target surface to the point of luminosity[1], an effect that may be highly undesirable if the target is a high explosive[2]. Collectively, these phenomena are referred to as shock wave precursors as they occur ahead of the shock front.

In this work, previously published literature on precursors is reviewed and followed by a presentation and discussion of several precursor effects that have been observed to occur in argon flashes at Los Alamos National Laboratory.

PREVIOUS LITERATURE

Prior research on this topic has determined that the surface behind a strong shock front can produce electromagnetic radiation and fast electrons, both of which are thought to drive the precursors. It is also thought absorption of this radiation by experiment walls can result in the release of photoelectrons. Typically, researchers have focused on measuring either the electron diffusion or the electromagnetic radiation that results from the shocked gas, but not both in the same study. The general conclusions are that electron diffusion has a more significant precursor effect in pressure-driven shock tubes at lower Mach numbers, while radiation is dominant at higher Mach numbers[3].

Boundary Layer Disturbance Precursors

Shreffler and Christian[1] published the first reference to shock wave precursors in 1954. They noted that when strong shock waves driven by Comp B were propagated through certain gases, a boundary disturbance would run up the shock tube wall some distance ahead of the main shock front. The disturbance would also run ahead of the main front on wires and other objects oriented with their long axis in the direction of shock propagation. Varying the material did not affect the growth of the disturbance. They concluded that radiation from the shock front that was incident on the shock tube walls created a preheated thermal boundary layer. The increased sound speed in this heated wall region supported a higher shock velocity, allowing the shock wave to run ahead of the main front in this region and create the boundary disturbance. They also noted that this radiative heating was strong enough that surfaces ahead of and parallel to the shock front were heated to incandescence and emitted secondary shock waves. For their driver conditions (8 mm/μs shock into a test gas at atmospheric pressure), air, butane-propane, and helium were not found to support any precursors whatsoever. Sulfur hexoflouride and 50% argon-50% nitrogen mixtures exhibited small disturbances, while chlorine mixtures and argon mixtures supported very prominent precursors.

Duff and Peterson[4] studied the evolution of these boundary precursors in argon mixtures driven by C-4 explosive. Experiments were carried out in 102 mm inner diameter (ID) aluminum tubes with length-to-diameter (L/D) ratios ranging from 1 - 8. The exterior tube walls were supported by detasheet with a detonation velocity of 7.2 mm/μs, which was slightly slower than the initial shock velocity in the argon of 7.5 mm/μs. This explosive supported wall was intended to prevent the severe attenuation observed in tests with inert walls. They found that the precursor first developed its maximum length at an L/D of 2, before decreasing in length and growing in

In Proceedings of the 13th International Detonation Symposium, pp. 1035–1044.

width. The shock width then seemed to grow asymptotically until the planar shock region was only 30% of the diameter of the tube.

Temperature and Irradiance Estimates

Several researchers have analyzed the light output of the argon flash in an effort to characterize the radiation flux emitted from the device. Vulliet[5] performed a theoretical analysis that involved calculating the shock temperatures in xenon, krypton, and argon when driven by Comp B explosive. He then estimated the irradiance that would be transmitted to a target located 1 m away from the shock front. For argon, the shock temperature and power flux were found to be 23,000 K and 1.4×10^{10} W/m^2. Values for xenon and krypton were somewhat higher but still the same order of magnitude as those of argon.

Conger et al.[6] propagated shock waves driven by small amounts of PETN and RDX into argon, measuring the light output in the infrared, visible, and ultraviolet regions with a spectrograph. They calculated that the argon shock emitted maximum radiation at a wavelength of 123 nm and inferred that the shock temperature was about 20,000 K by studying the ratio of UV to visible light that radiated from the front.

Taylor and Kane[7] also measured the visible spectra emitted from argon driven by a Comp B driver and determined that the gas radiated like a blackbody at a temperature of approximately 23,000 K.

Photoelectron Precursors

A large body of work has also been devoted to studying the diffusion of electrons ahead of strong shock waves. Work by Shafranov[8] showed that in a plasma with a shock, the electrons and ions may be at different temperatures. Due to the higher electron thermal conductivity, the electron temperature jumps up ahead of the shock while the ion temperature does not change by as much. Weymann[9], Groenig[3], and others[10–12] working with low-pressure argon shock tubes have determined that a precursor wave of fast electrons diffuses ahead of the shock wave. This wave may aid in the development of the disturbance observed by Shreffler and Christian[1] and Duff and Peterson[4].

ARGON SHOCK IN A TUBE

First, we discuss the boundary layer disturbance phenomena of a planar shock wave propagating in a cylindrical tube. A streak camera was used to view the light emitted from the window of an argon flash, allowing the wave interactions to be recorded as a function of time. The camera aperture had a narrow entrance slit to record only the light emitted along a diameter of the tube. The image of the entrance slit is swept along the film. Time increases in the vertical direction of the film while space along a tube diameter is represented in the horizontal direction.

Four shock tubes were photographed. Each tube was made of dural with an ID of 88.9 mm and a wall thickness of 6.35 mm. The tubes were of lengths 25.4 mm, 50.8 mm, 101.6 mm, and 152.4 mm. Each shock tube was driven by a plane detonation wave in a disk of PBX-9404 explosive that was 101.6 mm in diameter $\times$ 25.4 mm thick and was initiated by a 100 mm diameter plane wave lens. The disk drives the shock wave in the tube; the lens serves only to provide simultaneous initiation of the disk on one face. The explosive disk seals one end of the shock tube. The other end is sealed by a glass disk about 30 mm thick. The streak records for all four tubes are shown in Fig. 2.

At the bottom edge of the streak camera records, corresponding to the time when the detonation wave in the explosive reached the interface with the argon, we can see the light intensity rise to full brightness in about 0.1 μs (one small division). This rise time is the time needed to shock one or two optical depths of argon so that it radiates as a blackbody. The shock wave travels about 9 mm/μs, and the density of argon at one Los Alamos atmosphere (0.793 bar) is about 1.30×10^{-3} g/cm^3, so that in 0.1 μs about 1.17×10^{-3} g/cm^2 becomes optically thick. The compression of argon in the shock is about 12, so the layer responsible for the light is only about 75 μm thick. The striations in the light that persist for about 0.5 μs are caused by small imperfections in the wave from the explosive, amplified by the instability of the interface between the explosive gases and the argon. As the argon layer becomes thicker, the ripples lose their effect.

In a detonating explosive, the pressure is greatest at the detonation front and it falls rapidly in the gases following the front. As time goes on, the pres-

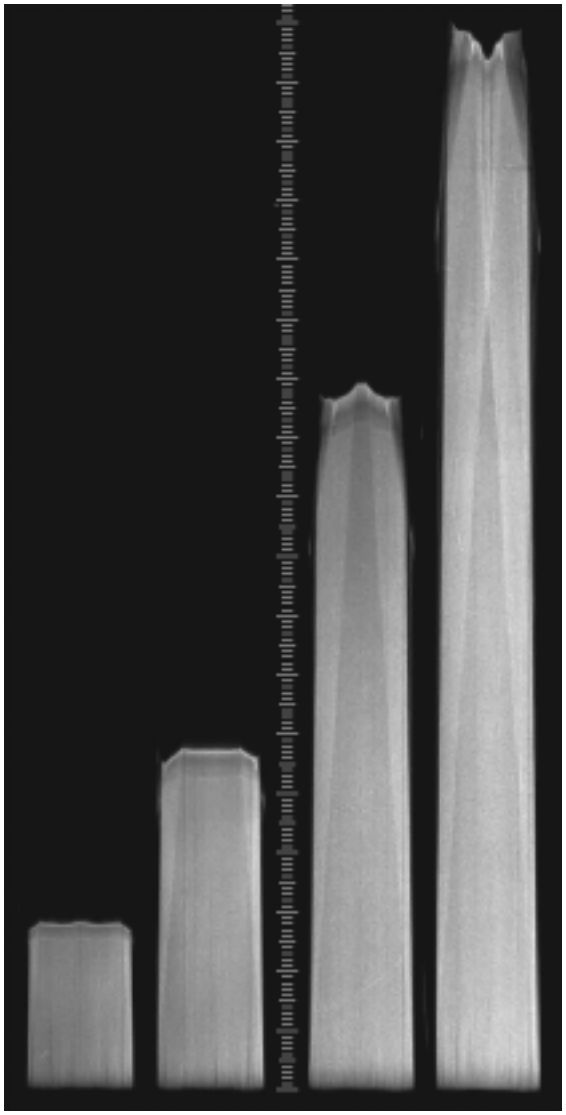

FIGURE 2. Streak records for the 25.4 mm, 50.8 mm, 101.6 mm, and 152.4 mm long tubes. Time marks are 1.0 μs for each large division, so the total length is about 19 μs. In the spatial direction, each tube is 88.9 mm in diameter and the width of the bright band at the bottom of each trace corresponds to that distance.

sure in the products driving the argon falls, and the wave slows slightly. Since the temperature depends on the shock speed, the shock temperature and shock brightness decrease with time. The decrease can be seen along the center of each tube, but only up to about 13 μs in the longest tube. The x-t data from the three tubes in which a plane segment of the main shock reaches the end window are fit fairly well over the range of x = 0 to 101.6 mm and t = 0 to 12.1 μs by

$$x = 697\left[1 - \exp\left(-0.013t\right)\right] \tag{1}$$

and the speed, obtained by differentiation, is

$$u = 9.06\exp\left(-0.013t\right) \tag{2}$$

with x in mm, u in mm/μs, and t in μs.

Radiation from the argon shock wave is absorbed at the tube boundaries. The window at the end of the tube is transparent only in the visible, and absorbs much of the radiation incident on it. The gas next to the window is heated and as it expands it drives a shock wave ahead of it back toward the main shock as has been observed in earlier studies[1]. The intersection of these two shocks can be seen in the short tube about a quarter of a microsecond before the light goes out, and in the next longer tube about one-half microsecond before the end. The light brightens for a brief instant, and then becomes dimmer than the original main shock. The reflected shock is moving back, and in the collision the pressure and temperature rise. At the high temperature, the gas becomes optically thick very quickly. Then the transmitted shock in the heated argon becomes less bright.

The end of each record shows what happens as the shock wave reaches the glass. The light brightens momentarily as temperature rises in the reflected shock, but it cools quickly. The precursor shock leads along the wall of the tube, and in the 50 mm ID tube arrives at the glass about 0.2 μs before the shock in the center. Figure 3 is a diagram of the structure near the wall. The heated layer at the wall is less dense than the bulk of the argon, and is hot so its sound speed is elevated. The main shock in the argon drives a shock at high speed into the hot gas, and a wave that looks like a Mach stem exists at intersection of the shocks. The pressure and temperature behind the Mach stem are elevated due to the intersection of the shocked flow from each shocks, resulting in brighter gas. In the streak records for the two longer tubes, the Mach stems can be seen converging toward the center, reaching it at about 13 μs in the longest tube. At convergence, the waves reflect off of each other, further increasing the postshock temperature and irradiance. The wave focusing also increases the local postshock pressure, which accelerates the velocity of the shock in the central region,

causing it to reach the glass early. After the interaction, the shock wave has a convex section at its center, surrounded by a funnel shaped shock. The cusp at the intersection of these waves shows up as a pair of dark lines in the streak.

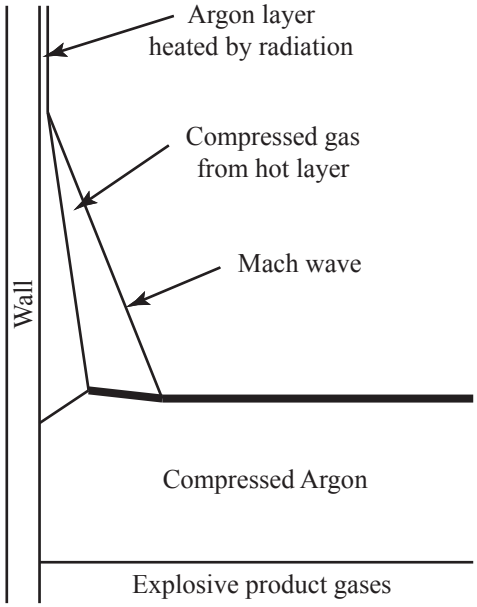

FIGURE 3. A sketch of the wave structure along the wall of the tube from Jones and Davis[13].

The oblique shock wave is much less luminous than the main shock wave and Mach stem, but it is still ionized enough to be opaque to the brighter gas behind it. As such, it appears as a dark growth along the wall that grows with time. In the streak record there are some narrow dark lines that are caused by defects in the camera slits. They are exactly parallel to the time direction. Looking carefully, one can see that the boundary is not the tube wall, but the darker oblique wave surface that appears to narrow the streak as time proceeds. The bright light from the aforementioned Mach stem (that is adjacent to the oblique wave) also grows with time and can easily be seen. Figure 4 (discussed below) shows several frames of the shock profile, better illustrating the growth of the Mach stem and the oblique wave. Note the difference in brightness of each component.

Although the precursor waves were studied by Shreffler and Christian[1], Jones and Davis[13], and others more than half a century ago, the details of the wall heating are still not resolved. The process has been attributed to simple radiant heating, to production of fast photoelectrons at both the shock front and tube walls, and to production of excited argon atoms, especially the metastable first excited state atoms. Probably all these processes and others are active to some degree.

FLOATING DROPS

Side on views of the shock wave profile were also obtained to view the growth of the wall precursors. During this study, however, a second type of precursor presented itself. The new precursor appeared as a small bubble or drop just ahead of the main shock wave. These "floating drops" remained just ahead of the shock surface, gradually growing in width.

A typical shot box for the experiments discussed next is shown in Fig. 4. The window is out in front of the region of interest so as to be little affected by the radiation. White photographer's cardboard with a mineral coating is directly opposite the window to reflect the light, providing a backlight. Extending the explosive to the window prevents the shock breakout from the HE from interfering with the pictures.

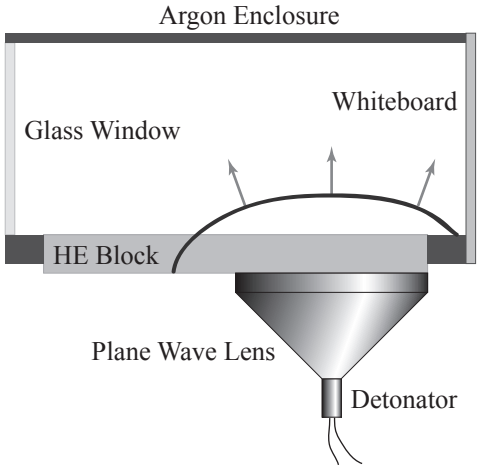

FIGURE 4. A sketch of the shot box used during the imaging of the floating drops. The camera was located to the left of the window.

Fig. 5 consists of four images of a shock in argon that were made using an image intensifier camera (I^2C) which has four independent cameras with the subject imaged on them through beamsplitters so that each camera has exactly the same view[14]. The

In Proceedings of the 13th International Detonation Symposium, pp. 1035–1044.

four cameras can be triggered independently, the exposure time can be set independently, and the gain can be set independently. For the pictures shown here, the exposure time for each camera was 30 ns.

The floating drops can clearly be seen a short distance ahead of the main wave. These small precursors grow very little, but do widen and follow the flow of the main shock as it expands at the edges. They have not been seen in pictures looking directly at the main shock as the contrast is very low. It may be that these small precursors are started by jetting from the explosive surface, or from small defects in the explosive, or from the multimaterial character of the explosive. We have no explanation for these floating drops and they have not been observed in any previous work.

PRECURSOR ON A TERMINATED WIRE

Precursors also form on a rod or wire placed orthogonal to the shock front. This phenomenon has been discussed in detail by many authors [1]. The precursors that form are independent of the material of the obstacle and do not appear to depend significantly on the obstacle size either. Of more immediate interest is the evolution of the precursor upon reaching the end of the wire. It is thought that this process provides insight into the growth of the floating drops.

The bottom frame of Fig. 6 shows the precursor on a stainless steel wire 25 mm long and 250 μm in diameter. The precursor grows and travels ahead of the main shock as expected. When it gets to the end of the wire it persists, but moves more slowly than the main shock. At late time it is not swallowed up by the shock, but decays in velocity and expands in width (Fig. 6, top frame). Similar experiments performed by Shreffler and Christian [1] provide more camera frames.

It appears that as the precursor reaches the end of the wire, its velocity drops below that of the main shock. The sudden removal of the radiation-absorbing surface illustrates the effect of wall heating on the sustenance of the disturbance. Now unsupported and propagating into a gas with no thermal gradient, the precursor's diffraction becomes more prominent. While this diffraction weakens the precursor and decreases its propagation velocity, the gas behind the diffracting wave is still hotter than the un-

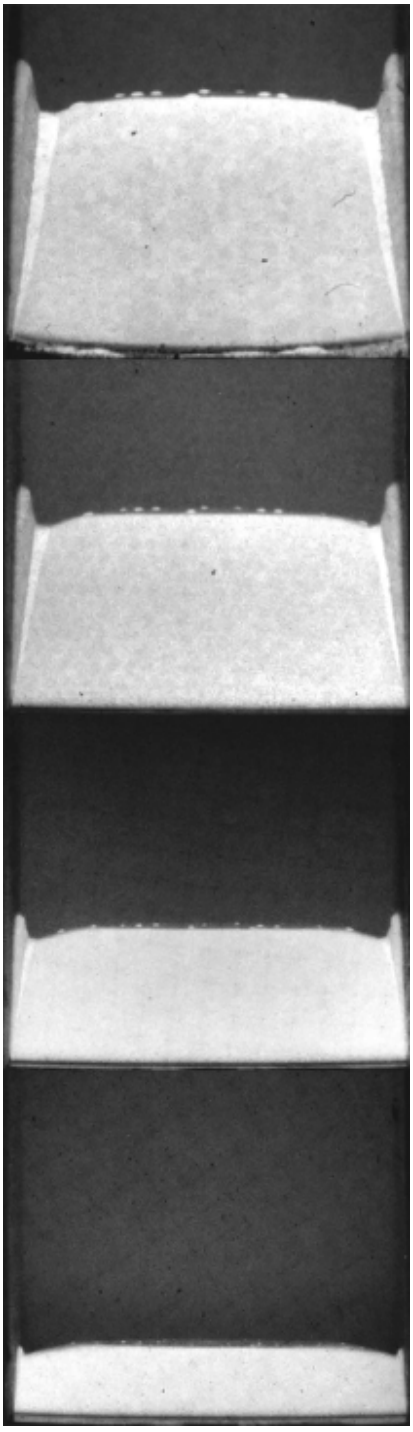

FIGURE 5. Images of "floating drops" ahead of a shock in argon. The growth of the oblique wave and Mach stems along the wall are also illustrated.

In Proceedings of the 13th International Detonation Symposium, pp. 1035–1044.

shocked argon, and the main shock accelerates into this region, slowing the rate of decay. In this fashion, the precursor changes from the spike-shaped object in the bottom frame of Fig. 6 to the pancake-shaped object at the top frame. Floating drop precursors, conveniently located alongside the wire precursors, appear to widen in a similar manner.

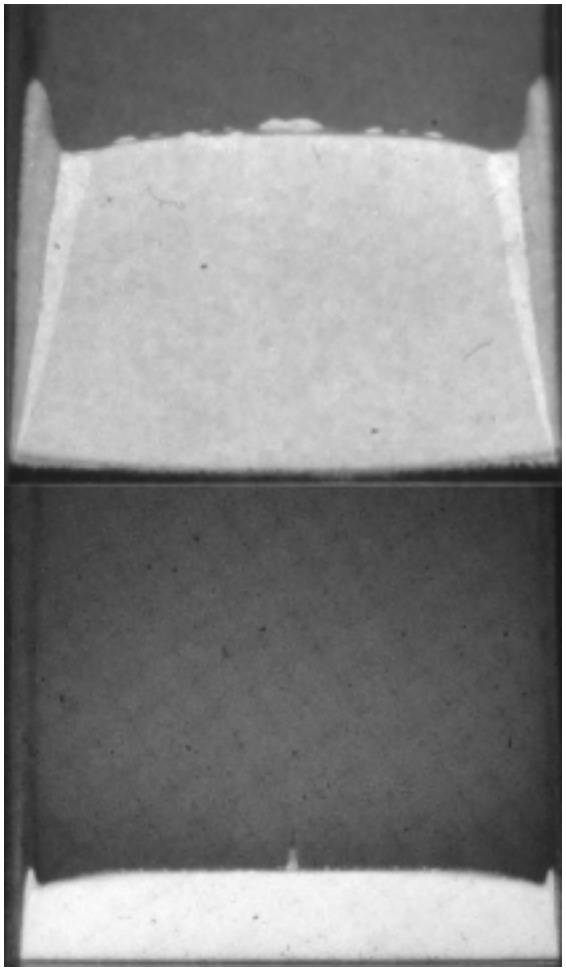

FIGURE 6. Images of the precursor propagating over a wire (bottom) and after the end of the wire (top).

WIRE PRECURSORS IN ARGON AND AIR

The work of Shreffler and Christian[1] has demonstrated that precursors do not occur in air at shock velocities of 9 mm/μs. It is, however possible to generate artificial precursors in air by creating a thermal gradient in the gas ahead of a strong shock wave. Figure 7 shows two images of a shock in argon with two tungsten wires perturbing the flow. Each wire was 25 μm diameter. The left-hand wire was held at the top and just reached the explosive surface. The right-hand wire was exploded about 35 μs earlier by a current pulse from a capacitor discharge unit; it was held near the explosive surface by a conductor. The precursor can be seen running up the unexploded wire. The right-hand precursor is a little behind the left-hand one, due to the fact that the wire did not go all the way to the explosive surface but only to an electrical conductor positioned slightly ahead of the surface of the explosive/argon interface. The shapes of the two precursors are somewhat different; the one along the exploded wire is larger in diameter and more blunt.

Fig. 8 shows an identical system except that the gas is air instead of argon. Note that there is no precursor on the left-hand wire, but a large one in the air heated by exploding the right-hand wire. The preheating of the air by the exploded wire yields similar results to the argon case, although the air is not as luminous. The wall disturbances are very small.

To confirm the hydrodynamic basis for the observed precursor shocks, a simulation of a planar air shock impinging on a column of low density air was performed. Air was chosen to make the comparisons since we believe radiation effects in it are negligible. To replicate the experiment of Fig. 8, a planar shock of speed U_s = 8.07 mm/μs was allowed to impinge on a 3 mm radius of air which has been expanded to a volume 16 times that of the surrounding quiescent air. A Mie-Gruneisen equation of state based off of a linear Hugoniot was chosen to model the air[15]: U_s = 0.2375 mm/μs + 1.0575 U_p with the ambient air having ρ_0 = 1.01 $\times 10^{-3}$ g/cm^3 and a Gruneisen parameter Γ_0 = 0.4, with $\Gamma\,\rho = \Gamma_0\,\rho_0$. The simulation results with a spatial resolution of Δx = 0.0625 mm are presented in Fig. 9 along side the experimental photographs.

As can be seen in Fig. 9, a precursor shock in the low density air leads the main air shock. This is caused by a combination of high sound speed in the column of air along with the fact that the post shock state in the column is at a lower pressure than the surrounding post shock state, and thus the high density and pressure air has a tendency to be drawn into the column area, which further supports the precursor shock wave. The contact wave between the

In Proceedings of the 13th International Detonation Symposium, pp. 1035–1044.

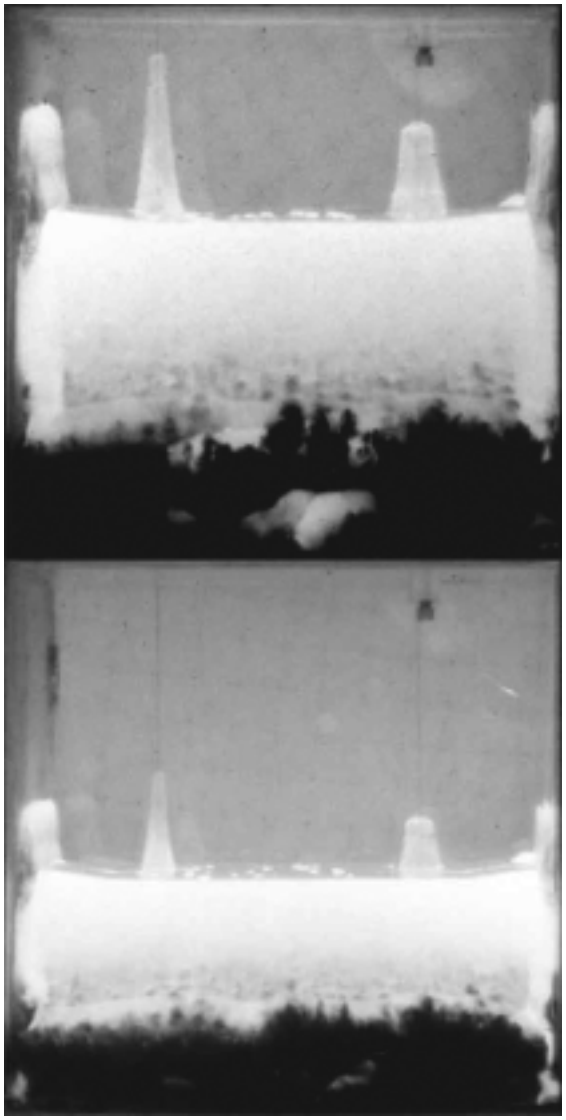

FIGURE 7. Images of a shock wave propagating in argon. The right wire was exploded 35 μs prior to the shock breakout.

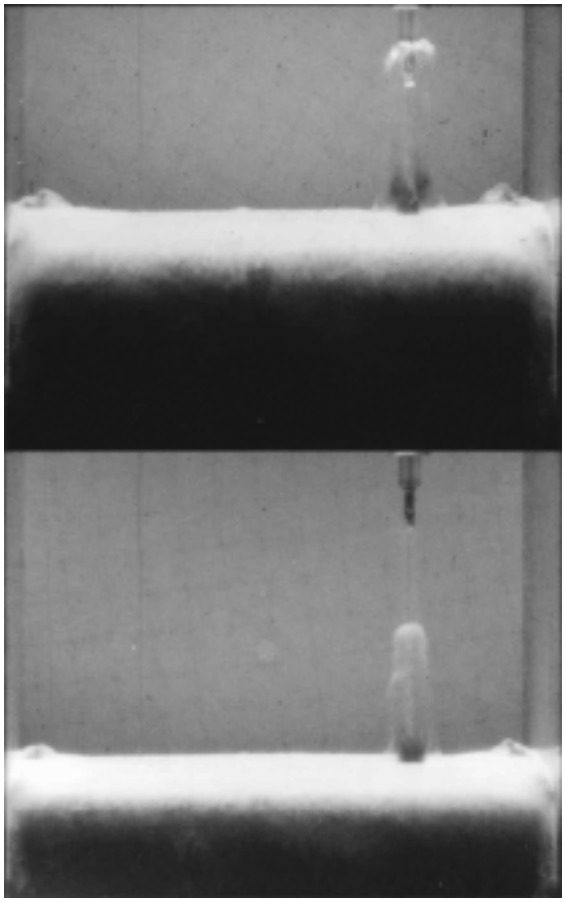

FIGURE 8. Images of a shock wave propagating in air. The right wire was exploded 35 μs prior to the shock breakout. Note the absence of any floating drop precursors in the air.

shocked ambient air and shocked low density air can be clearly seen; the "white" in the plot of p/ρ is the shocked low density air, while the light gray is the ambient shocked air.

While the exploding wire does not accurately recreate the exact temperature profile and thus, the exact shape of the argon precursor, qualitatively it emulates the phenomenon. This demonstrates that the gas dynamics of precursor formation are independent of the mixture and only dependent on sound speed and density gradients. However, while the argon is able to generate the thermal gradient ahead of the shock front from the radiation it would appear the air mixture is not. This is expected for two reasons. First, the shocked air does not reach as high a temperature (12,000–15,000 K) as the argon for a given shock strength due to its higher value of specific heat. Second, the oxygen and nitrogen composing air both strongly absorb hard UV radiation. Thus, what little UV radiation is emitted from the front is promptly absorbed by the unshocked gas, before it can heat material surfaces.

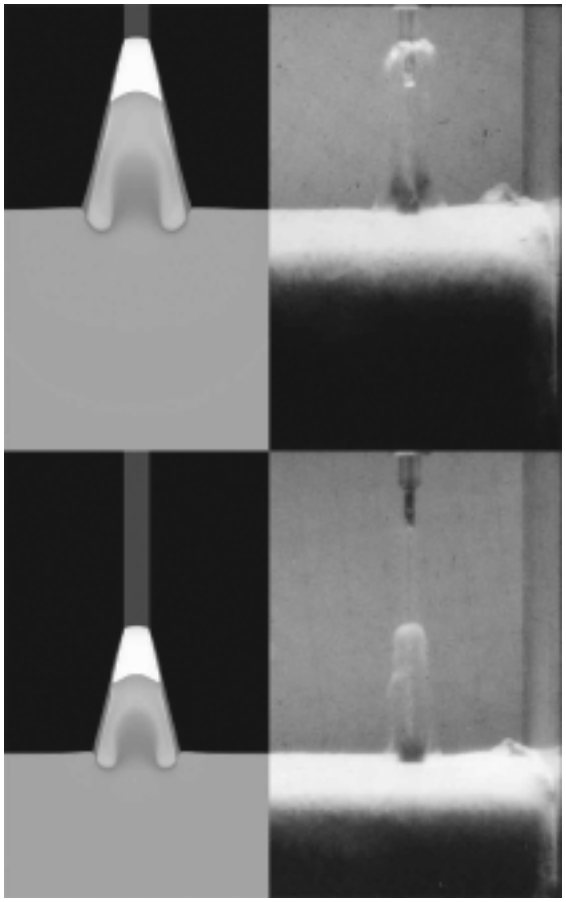

FIGURE 9. Computational plot of p/ρ (left) and experimental photograph (right) at two times separated by 3 μs.

NUCLEAR EXPLOSION FIREBALL

Images obtained from nuclear explosions in air show features that look like wire precursors and floating drops. Fig. 10 is a photograph of a nuclear explosion fireball at early time. During this test (which was not performed by the authors), a nuclear device was elevated above the ground by a balloon. Precursors (called spikes) run along the support cables tethering the balloon and look like the precursors on the wires in Figs. 6 and 7. The surface is marked by small bright precursors referred to as "measles" which may be analogous to the floating drops seen in Fig. 5. While the physics of the heating processes that lead to the precursors is very different from that of the argon shock, perhaps the gas dynamics of the shock wave in the air are similar. In the very strong shock from the nuclear explosion there is an absorbing layer[16], caused by radiation, ahead of the luminous region. Perhaps the measles are regions where the absorbing layer is thinner than in other regions, so the light is brighter. Alternatively, perhaps in some regions the absorbing layer was thicker and preferentially absorbed more radiation, allowing portions of the shock to run ahead of the main wave, as the spikes do.

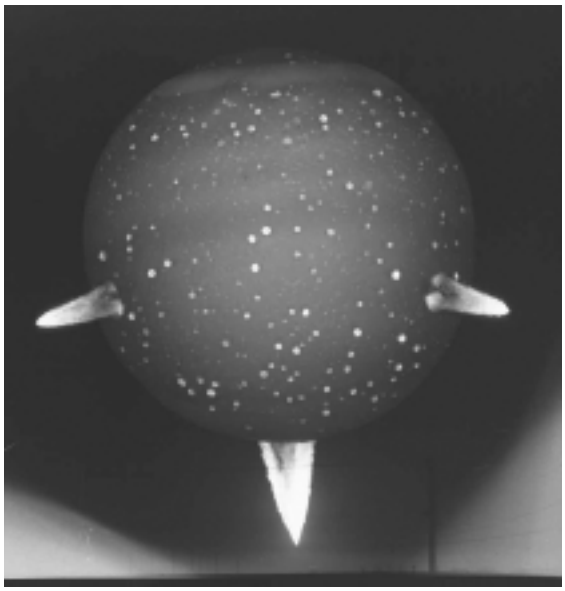

FIGURE 10. Image of a shock wave from a nuclear explosion test named "Plumbob Priscilla." This test had a yield of 37 kT and was performed on June 24, 1957. Frame identifier number J10F-5066, courtesy of Los Alamos National Laboratory.

CONCLUSIONS

Observations of precursors in argon, including the formation of boundary layer disturbances and floating drops on the surface of the shock front, have been presented and discussed. While precursor effects are typically not observed in air at the shock speeds tested in this study, artificial precursors were created by using an exploding wire to create a thermal gradient in the gas ahead of the shock front. This confirms that the radiation transfer from the hot shocked gas to material walls and the subsequent transfer of this heat into the gas ahead of the shock is a necessary requirement for precursor formation. It is thought

that due to its lower specific heat value and better transparency in the UV spectrum, argon was better able to generate the thermal gradients ahead of the main shock wave needed for precursors to occur. Air, on the other hand, did not generate sufficient thermal gradients for precursors due to its higher specific heat and opacity to hard UV radiation. However, the nuclear test shown indicates that the generation of precursors in air is indeed possible with a strong enough shock and enough radiation.

Researchers working with strong shocks in noble gases should be aware of these precursor effects. Future work will attempt to determine the details of the gas heating associated with precursor formation and the source of the floating drops.

ACKNOWLEDGEMENTS

The authors would like to acknowledge discussions with D. Moore on the topics of air opacity in the hard ultraviolet and possible precursor generation mechanisms.

REFERENCES

1. R. G. Shreffler and R. H. Christian. Boundary disturbances in high-explosive shock tubes. *Journal of Applied Physics*, 25(3):324–331, 1954.
2. J. Roth. Initiation of lead azide by high-intensity light. *The Journal of Chemical Physics*, 41(7):1929 – 1936, 1964.
3. H. Groenig. Precursor photoionization and electrons. *The Physics of Fluids*, 6(1):142–144, 1963.
4. R. E. Duff and F. I. Peterson. Shock precursor observations. *Journal of Applied Physics*, 51(7):3957–3959, 1980.
5. W. G. Vulliet. Radiation from explosive-driven shocks in the noble gases. *Journal of Quantitative Spectroscopy and Radiative Transfer*, 4:839–845, 1964.
6. R. L. Conger, L. T. Long, J. A. Parks, and J. H. Johnson. The spectrum of the argon bomb. *Applied Optics*, 4(3):273–276, 1964.
7. W. H. Taylor, II and J. W. Kane, Jr. Radiant properties of strong shock waves in argon. *Applied Optics*, 6(9):1493–1495, 1967.
8. V. D. Shafranov. The structure of shock waves in a plasma. *Soviet Physics JETP*, 5(6):1183–1188, 1957.
9. H. D. Weymann. Electron diffusion ahead of shock waves in argon. *The Physics of Fluids*, 3(4):545–548, 1960.
10. D. L. Jones. Precursor electrons ahead of cylindrical shock waves. *The Physics of Fluids*, 5(9):1121–1122, 1962.
11. R. Matsuzaki. Further note on the precursor wave. *Japanese Journal of Applied Physics*, 4:236–237, 1965.
12. M. J. Lubin and E. L. Resler, Jr. Precursor studies in an electgromagnetically driven shock tube. *The Physics of Fluids*, 10(1):1–8, 1967.
13. C. R. Jones and W. C. Davis. Optical properties of explosive-driven shock waves in noble gases. *Proceedings of the Los Alamos Conference on Optics*, 380:312, 1983.
14. O. G. Winslow, W. C. Davis, and W. C. Chiles. Multiple exposure image-intensifier camera. *The Proceedings of the 6th International Detonation Symposium*, pages 664–667, 1976.
15. W. E. Deal. Shock hugoniot of air. *Journal of Applied Physics*, 28(7):782 – 784, 1957.
16. Ya. B. Zel'dovich and Yu. P. Raizer. *Physics of Shock Waves and High-Temperature Hydrodynamic Phenomena*. Dover Publications, 2002.